Journal of Materials and Electronic Devices 5 (2023) 9-13

JOURNAL OF MATERIALS AND ELECTRONIC DEVICES
FYTRONIX JMED http://dergi-fytronix.com/

Superconductivity in $NdBa_2(Cu_{3-x}Mg_x)O_{7+z}$ High Temperature superconductor system

Kübra Yakıncı*

Iskenderun Technical University, Faculty of Engineering and Natural Sciences, Department of Basic Engineering Sciences, 31200-İskenderun, Hatay-TÜRKİYE

Today, many scientists work intensively on the development of new high-temperature superconductors or applications. In this context, it is not surprising that a new superconductor is discovered every year at a high or low-temperature scale. It is known that NdBaCuO-based superconductors show a transition to superconductivity around 96 K, which was found a long year ago. At the same time, a large number of substitutions or doping have been made on this material, mainly in the Cu site. However, no study was found with Mg doping or substitutions instead of Cu site in the NdBaCuO system. In this study, for the first time in the literature, $NdBa_2(CuMg)_3O_{7+z}$, where x=0.1%, 0.2%, and 0.3%, materials were prepared with a solid-state reaction method and then characterized. In the first analysis, it was found that the material passed into the superconducting phase at 98 K and had a critical current density of the order of 10^6 A/cm^2 at 4.2 K. The results of other characterizations along with crystal parameters and magnetic properties are presented in this study.

Keywords: *High Tc superconductors, $NdBa_2(Cu_{3-x}Mg_x)O_{7+z}$, superconductors,*

Submission Date: 12 October 2023
Acceptance Date: 03 December 2023

**Corresponding author: kubra.yakinci@iste.edu.tr*

1. Introduction

NdBaCuO superconductors have been known for many years as one of the materials that can be used in many areas of superconducting technology. However, it still needs some improvements. For example, for such superconductors to be widely used in technology, they are expected to have a higher critical transition temperature, T_c, value, and most importantly, a higher current carrying capacity, J_c, and more stability even in a high magnetic field. Compared to YBCO superconductors, NdBaCuO materials are known to have some important properties such as at least 9 times less oxygen partial pressure, higher pinning ability and therefore higher critical current carrying capacity, and a slightly higher critical transition temperature [1-10]. In addition, they are very suitable for spintronic device applications as well. These features make it worth doing more extensive research on NdBaCuO superconductors.

NdBaCuO superconductor material has an orthorhombic crystal system and unit cell parameters are determined as a=3.8621 Å, b=3.9180 Å, c=11.7713 Å and accordingly, the unit cell volume is 178,122 Å^3 [7]. The T_c is ~ 96 K and the J_c of bulk materials is higher than 10^6 A/cm^2 at 4.2 K and under zero field [8]. However, in the NdBaCuO material, the Nd-Ba reaction can cause significant changes in the T_c as a result of the formation of different solid solution phases and large changes in the nominal phase composition [7-9]. Therefore, maximum care must be taken when preparing the material. However, when NdBaCuO is prepared especially at low oxygen pressure, these drawbacks can be avoided and can be a sharp transition to the superconducting phase obtained.

In this study, superconducting $NdBa_2(Cu_{3-x}Mg_x)_3O_{7+z}$ materials, where x=0.1%, 0.2%, 0.3%, 0.4% and 0.5%, were prepared with conventional solid-state reaction method and then characterized. In the analysis, it was found that the material had a metallic behavior up to the transition point and then transferred into the superconducting phase sharply at ~98 K and had a J_c of the order of 10^6 A/cm^2 at 4.2 K. The results of other characterizations along with crystal parameters and magnetic properties are presented in this study.

2. Experimental

Superconducting $NdBa_2(Cu_{3-x}Mg_x)_3O_{7+z}$ materials, where x=0.1%, 0.2%, 0.3%, 0.4% and 0.5%, were prepared with conventional solid-state reaction method. For the preparation of the material, we used high purity Y_2O_3 99.99 % (Sigma-Aldrich), BaCO 99.99 % (Sigma-Aldrich), CuO 99.99 % (Sigma-Aldrich), and MgO 99.99 % (Sigma-Aldrich). The mixed raw powders were first calcined at 880°C for 24h in the air twice with intermediate grinding. Then re-mixed powders were pelletized at 8 tons of pressure at room conditions. The pellets were then heated at 1070°C for 45 minutes and then slowly cooled to 950°C within 2h at 1% O_2 in Ar gas. Samples were then cooled to 500°C and annealed for 30 h in a 100 % O_2 atmosphere.

For the characterization of the prepared samples, we used an X-ray diffraction (XRD) analysis for structural investigation. XRD experiments were done with a 2°C/min scan rate using the Malvern-Panalytical Empyrean system and Cuk_α radiation between 2θ=3-80°. The structural parameters were calculated by using the least-squares fit of the XRD lines and then the Rietveld refinement program was applied. A Quantum Design Physical property measurement system, PPMS-8T, with Vibrating Sample Magnetometer, VSM, attachment, for electrical and magnetic properties under ± 8 T magnetic field. A homemade *I-V* measurement system at 77 K was also used for further characterizations of the samples produced.

3. Results and Discussions

The XRD graphs of the samples prepared are given in Fig.1a-d and also calculated values of the unit cells are given in Table 1. Initially, we did not obtain any impurity phase in pure and 0.1% Mg-substituted samples. However, for 0.2% and 0.3% Mg-substituted samples. It was observed that the XRD peaks in the unsubstituted and 0.1% Mg-substituted samples were almost the same, but in the 0.2 and 0.3% Mg-substituted samples, MgO and MgO contaminated phases such as MgCuO impurities were obtained, Fig.1.

Table 1. Calculated unit cell parameters of the samples.

Samples	Lattice parameters, Å			
	a	b	c	Unit cell volume, Å^3
Pure	3.8621	3.9180	11.7713	178.122
0.1% Mg	3.8609	3.9171	11.7691	177.99
0.2% Mg	3.8601	3.8955	11.7684	176.96
0.3% Mg	3.8572	3.8925	11.762	176.59

In addition, together with the substitution the peaks obtained were shifted slightly towards the larger angles.

This indicates that the MgO substitution can be incorporated with the NdBaCuO material. Accordingly, the calculations made indicate that lattice constants decrease by increasing the Mg substitution rate. The reason for this is explained as the ionic/atomic radius of Mg which is larger than the Cu ions. For the calculations of the unit cell parameters, we obtained a slight decrease in the a, b, c, and cell volume parameters, Table 1. This also indicates the incorporation of the MgO material with the NdBaCuO material itself. Unfortunately, we did not analyze the higher MgO substitution cases due to the deformed and multiphase nature of the main NdBaCuO structure. However, it is still under investigation in our laboratory.

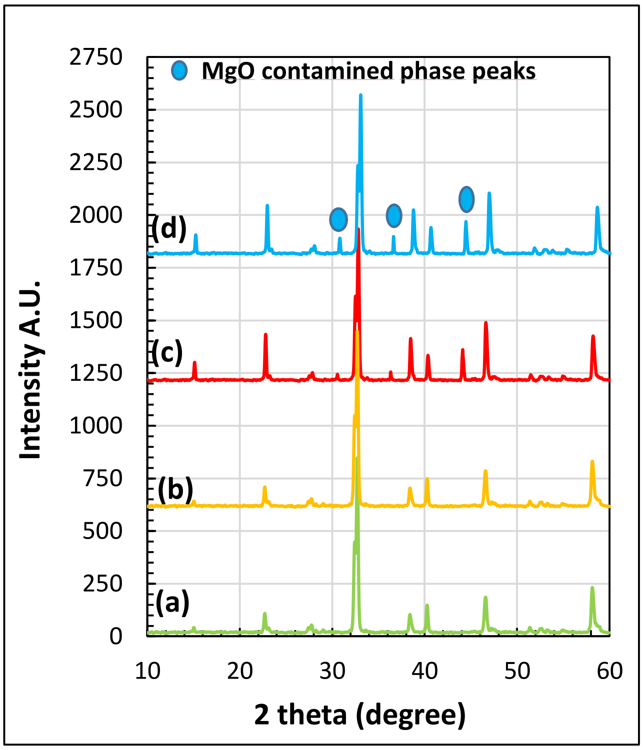

Fig.1. XRD graphs of the samples prepared. (a) Pure, (b) 0.1% Mg, (c) 0.2% Mg and (d) 0.3% Mg-substituted sample.

The electrical properties of the samples were made between room temperature and 90 K. The resistance versus temperature graphs of the samples prepared are given in Fig.2. It has been found that as the rate of Mg substitution instead of Cu in the NdBaCuO structure is increased, the normal state resistance of the material increases systematically. However, when the ratio was increased further after 0.3%, it was observed that the resistance increased excessively and exceeded the limits of the measurement system and superconductivity was disrupted. Therefore, 0.3% Mg substitution is considered to be a limit value for the superconducting properties.

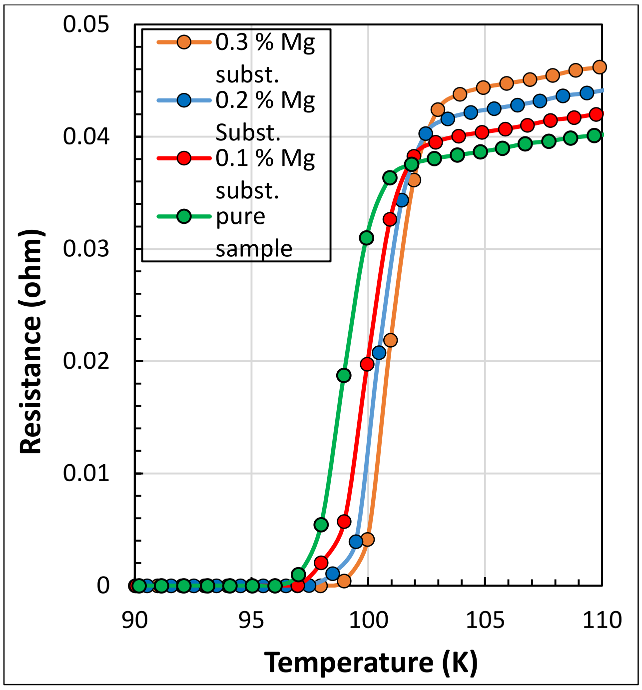

Fig.2. Resistance versus temperature measurements of the samples prepared

Thus, the best superconducting transition was obtained from the sample with 0.3% Mg substitution. It is considered that as the substitution rate increases, the normal state resistance increases and the disappearance of superconductivity after 3% substitution rate is due to the increase in impurity phases and therefore the increase in the scattering mechanism. As seen in Fig.2 the best T_{zero} value was obtained to be 98K for 3% Mg substituted sample which is approximately 2K better than the pure sample. 97 and 96 K T_{zero} values were obtained for 1%, 2%, and pure samples respectively. Resistance versus temperature measurements behavior of the 0.3% Mg substituted sample, which has the best sample, under magnetic fields of 0, 2, 4, 6, and 8 Tesla, (*MR-T*), are shown in Fig.3 as an example. The other superconducting samples showed similar trends after the measurements.

The results obtained reveal that there is no different feature from the conventional Type-2 superconductivity behavior with Mg substitution. Both the T_c and T_{zero} values were degreased when the applied magnetic field was increased as obtained in other High-T_c superconductor samples. Similar behavior is also obtained in all superconductor samples produced in this work. This showed that the substitution of Mg has no visible effect on the superconductivity behavior of the sample, but superconducting performance such as T_c value is increased by approximately 2K in the 3% Mg substituted sample. This could be due to the improvement in the grain boundaries of the material and due to the less scattering effect.

The magnetic properties of the samples were checked by using the magnetization versus applied field (*M-H*)

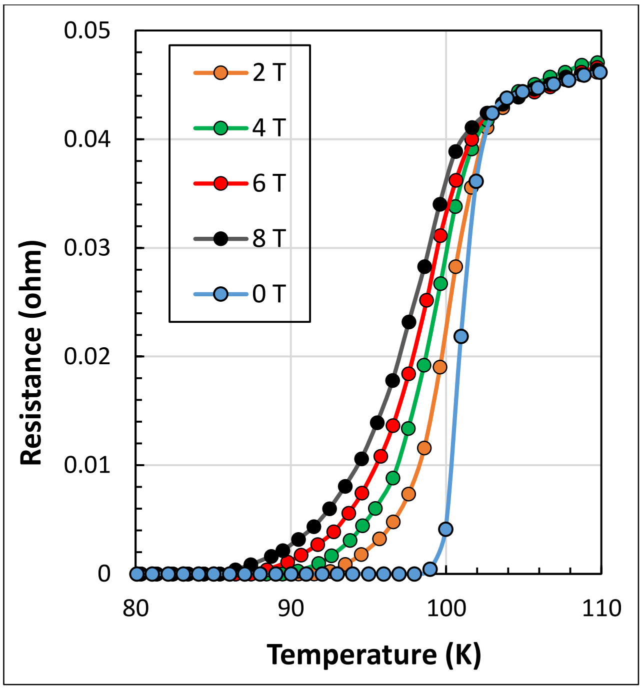

Fig.3. *MR-T* measurements of $NdBa_2(Cu_{3-x}Mg_x)_3O_{7+z}$ superconductor sample under Magnetic field.

measurements. The *M-H* curves of the samples prepared at 4.2 K are given in Fig. 4. The figure shows the change in the magnetization when the applied field increased. In general, very smooth *M-H* curves were obtained for Pure, 0.1%, 0.2%, and 0.3% Mg-substituted samples. This observation also suggests a type-2 superconductor performance and showed similar classical YBCO High-T_c superconductor peculiarity. However, this uniform magnetic peculiarity disappeared at high MgO contribution rates, for example; It was observed that the 0.5% Mg substituted sample diamagnetic properties completely disappeared and ferromagnetic behavior dominated the sample.

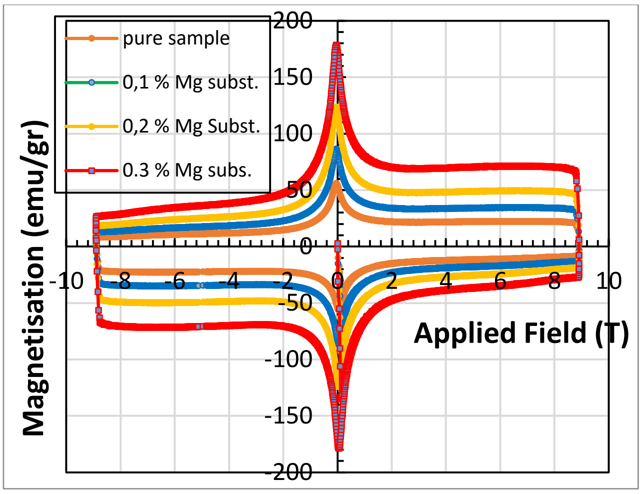

Fig.4. Magnetization versus applied field (M-H) measurements of the superconducting samples.

However, our studies and experiments continue why this show such a significant change even with a very small substitution rate. For the calculation of the magnetic field-dependent critical current density (J_c^{mag}), we used *M-H* loops of each sample and Bean's model, and results obtained at 4.2 are presented in Table 2. According to Bean's model [11],

$$J_c^{mag} = 20\frac{\Delta M}{a(1-\frac{a}{3b})} \quad (1)$$

where *a* and *b* are the length of the sample cross-section in cm ($a < b$), and ΔM is the difference between the magnetization measured with decreasing and increasing applied field in emu.cm^{-3}. As seen in Table 2 calculated J_c^{mag} results reveal that samples with Mg-substituted instead of Cu can carry 2-3 times more current than un-substituted pure samples. This result could be due to the modifications in the grain boundaries of the material. In addition, maybe MgO and a small amount of MgO-related impurity phases or clusters in atomic scale behave as pinning points in the material, and that positively affected the current carrying capability of the samples under the applied magnetic fields. This reveals that this material may have many different uses in the many high technology fields.

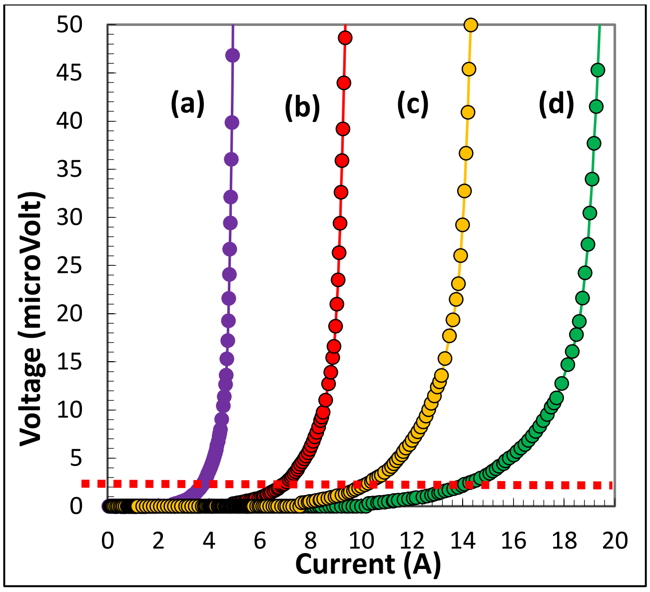

Fig.5. *I-V* measurement results of (a) pure, (b) 0.1% Mg, (c) 0.2% Mg, and (d) 0.3% Mg substituted samples.

We also measure the *I-V* properties of the actual samples using the PPMS system. The *I-V* measurements were done at stable 77 K. The samples were neatly cut in rectangular form of 1 x 3 mm and the measurements were taken at a constant temperature value and without applying any field. Current densities were calculated by considering the international scale (1 microvolt) and the results obtained are presented in Table 2. It was observed that as the MgO substitution ratio increased in the samples, the critical current density value also increased. Accordingly, the highest J_c value was obtained in the 0.3% Mg substituted sample with a value of 733 A/Cm^2, Table-2, which is

Table 2. Critical Current Density, J_c and J_c^{mag} values of the superconductor samples prepared in this work.

Sample	J_c at 77 K A/cm^2	J_c^{mag} at 4.2 K A/cm^2
Pure	288	1.88x10^6
0.1% Mg	395	2.4x10^6
0.2% Mg	586	3.6x10^6
0.3% Mg	733	5.1x10^6
0.4% Mg	No SC.	No SC.
0.5% Mg	No SC.	No SC.

approximately 2 times higher than the pure $NdBa_2Cu_3O_{7+z}$ sample. This result was found to confirm the critical current density, J_c^{mag}, results previously calculated by using the *M-H* data. This suggests that the grain connectivity could be modified by the MgO substitution and better J_c values then be obtained. However, we did not measure the higher MgO concentration cases such as 0.4% and 0.5% MgO substituted samples due to their non-superconducting nature.

4. Conclusions

In preliminary studies, Mg was successfully substituted to the NdBaCuO superconductor system instead of Cu at 0.1, 0.2, 0.4 and 0.5%. The results obtained show that the superconducting structure is disrupted after 0.3% Mg substitution rate. A multiphase NdBaCuO structure with more than 6 different non-superconducting phases emerged and superconducting properties diminished. This emerged as a critical limit value for Mg substitution instead of Cu. It was observed that there was a slight increase in the superconductivity transition temperature, T_c, value (~2 K) for the best sample which is 0.3% Mg substitution rate. However, our preliminary studies have shown that the main increase occurs in critical current density, J_c, values and that there may be an increase of at least 2-3 times compared to pure samples. Finally, results obtained reveal that the prepared materials can be easily produced on an industrial scale and, accordingly, can compete with other superconducting systems in technological use.

References

[1] F. Zhanguo, G. Weiying, L. Fenghua, W. Jue, S. Deahua, Preparation of NdBaCuO superconductor by zone-melting under low oxygen partial pressure, Physica C: Superconductivity, 386 (2003) 241–244 https://doi.org/10.1016/S0921-4534(02)02135-4.

[2] M. Salluzzo, A. Andreone, A. Cassinese, R. Di Capua, M. Iavarone, M.G. Maglione, G. Pica and R. Vaglio IEEE Transactions On Applied Superconductivity, Vol. 11, No. 1, March 2001, 3201-3212.

[3] I. Monot a, F. Tancret, P. Laffez, G. Van Tendeloo, G. Desgardin, Microstructure and properties of oxygen controlled melt textured NdBaCuO superconductive ceramics, Materials Science and Engineering B65 (1999) 26–34. https://doi.org/10.1016/S0921-5107(99)00193-2.

[4] W. Bieger, G. C-abbes, P. Schgtzle, A. Leistikocv, J. Thomas, P. Verges, microstructure and improved properties of NdBaCuO bulk materials, Materials Science and Engineering B53 (1998) 100-103. https://doi.org/10.1016/S0921-5107(97)00310-3.

[5] N. Kozhikuka, Physica C., 364-365 (2001) 320-3256

[6] E. H. Sujionoa, A. H. Khatimaha, A. N. Hasanaha, N. F. Mahendia, M. Y. Dahlana, N. A. Humairaha, A. Irhamsyaha, Nd(Fe)0.3Ba1.7Cu3O7-δ Oxide Material Crystal Structure and Morphological Analysis, Materials Today: Proceedings, 13 (2019) 264–269. https://doi.org/10.1016/j.matpr.2019.03.225.

[7] E.H. Sujiono, M. Muharram. 2017. Patent No. P00200800471 Reg. No. 44719.

[8] F. Tancret, I. Monot, P. Laffez, G. Van Tendeloo, G. Desgardin. Preparation and characterization of melt textured $NdBa_2Cu_3O_{7-\delta}$ bulk superconducting ceramics, Phys. J-Appl. Phys. 1(1998)185-190. 10.1051/epjap:1998135.

[9] M. Kakihana., N.N. Oleynikov, Y.D. Tretyakov. Physica C.340(2000) 32.

[10] D. M. Gokhfeld, S. V. Semenov, I. V. Nemtsev, I. S. Yakimov, D. A. Balaev, Journal of Superconductivity and Novel Magnetism 35 (2022), 2679–2687.

[11] Q.P. Ding, S. Mohan, Y. Tsuchiya, T. Taen, Y. Nakajima, T. Tamegai, Supercond. Sci. Technol. Low-temperature synthesis of $FeTe_{0.5}Se_{0.5}$ polycrystals with a high transport critical current density (2011). https://doi.org/10.1088/0953-2048/24/7/075025.